Study of the Coherent $\bar{p}d \to \bar{n}d\pi^-$ Reaction at 5.55 GeV/c

H. Braun, A. Fridman, J.-P. Gerber, A. Givernaud,* P. Juillot, J. A. Malko,† G. Maurer, and C. Voltolini
Laboratoire de Physique Corpusculaire, Centre de Recherches Nucléaires de Strasbourg, Strasbourg, France

W. A. Cooper‡
Argonne National Laboratory, Argonne, Illinois 60439

(Received 10 April 1973)

Based on 150 000 photographs an analysis of the $\bar{p}d \to \bar{n}d\pi^-$ reaction is presented. Cross sections for all the coherent channels obtained from this exposure are also given. The interpretations of the $\bar{n}\pi^-$ enhancement at $M_{\bar{n}\pi} \sim 1.3$ GeV/c^2 and the d^* bump at 2.16 GeV/c^2 observed in the $\bar{p}d \to \bar{n}d\pi^-$ reaction are discussed. Peripheral-type models are used in order to describe some production features of the $\bar{p}d \to \bar{n}d\pi^-$ reaction. The diffraction-dissociation aspect of the present data is discussed. Helicity conservation in the s or t channel is tested for the $\bar{p}d \to \bar{n}d\pi^-$ channel and also for the $\bar{p}d \to \bar{p}d\pi^+\pi^-$ and $\bar{p}d \to \bar{N}d3\pi$ reactions.

I. INTRODUCTION

In this paper we present an analysis of the $\bar{p}d \to \bar{n}d\pi^-$ reaction at 5.55 GeV/c incident momentum. The present data are extracted from a 150 000-photograph exposure taken at the Zero Gradient Synchrotron with the 30-in. bubble chamber.

The event selection, complicated by a contamination of $\bar{p}d \to \bar{p}d\pi^0\pi^0$ events, is discussed in Sec. II. In Sec. III we present some details on the calculation of the $\bar{p}d \to \bar{n}d\pi^-$ cross section, the latter being compared with all the coherent cross sections obtained from this exposure. Here, we define as coherent reactions those having a deuteron in the final state.[1]

In the $\bar{p}d \to \bar{n}d\pi^-$ channel we observed the so-called $N^*(1300)$ enhancement and copious d^* production. These features are discussed in Sec. IV. We have also attempted to investigate whether the $\bar{n}\pi^-$ enhancement at ~1.3 GeV/c^2 can be explained as arising from a specific production mechanism. To this end we considered peripheral-type models (Sec. V), where the free parameters were fitted to our data.

Finally, in Sec. VI we discuss the diffraction-dissociation aspect of our data. We also examine the compatibility of our data with helicity conservation in the s or t channels.

II. SELECTION OF EVENTS

After checking the compatibility of the calculated and observed track ionization and resolving the ambiguity between various competing reactions, we obtained a sample of event candidates for the $\bar{p}d \to \bar{n}d\pi^-$ reaction. Imposing a 3% χ^2 probability cut, we are left with 786 events.

The study of these 786 events shows that this sample is contaminated by other reactions. This can be seen in particular from the distribution of the laboratory momenta of the fitted π^- (P_π^{lab}), which shows an abnormal accumulation of events in the $P_\pi^{\text{lab}} > 3$ GeV/c region. From a study of Monte Carlo events we were able to attribute this accumulation to a contamination by $\bar{p}d \to \bar{p}d\pi^0\pi^0$ events. This last reaction was simulated by generating such events according to a peripheral e^{bt_d} law. Throughout this work t_d will always denote the four-momentum transfer between the initial and outgoing deuteron, whatever the coherent reaction will be. For the slope b characterizing the coherent production feature, we took the value $b = 16.8$ (GeV/c)$^{-2}$ obtained from the fitted $\bar{p}d \to \bar{p}d\pi^+\pi^-$ channel.[2] We then calculated for the faked $\bar{p}d \to \bar{p}d\pi^0\pi^0$ events the effective mass that the neutral system would have when we attribute the π^- mass to the outgoing $\bar{p}$. We observed that, for laboratory momenta of the negatively charged particles greater than 3 GeV/c, the mass of the calculated neutral system clusters around the $\bar{n}$ mass. These events can thus fit the $\bar{p}d \to \bar{n}d\pi^-$ hypothesis populating however the $P_\pi^{\text{lab}} > 3$ GeV/c region.

In order to eliminate this contamination, a cut of $P_\pi^{\text{lab}} > 3$ GeV/c was applied on our data, leaving us with a final sample of 595 events. To estimate the number of events lost by this cut we used the double-Regge model described in Sec. V. This model gives a good description of the experimental data and is then expected to give a realistic estimation of the number of events which are in the $P_\pi^{\text{lab}} > 3$ GeV/c region. We find that the losses due to our P_π^{lab} cut are about 27 ± 7 events. In Fig. 1(a) we show the region of the $\bar{n}d\pi^-$ Dalitz plot in which the losses occur. As can be seen from this figure these losses will not affect the $\bar{n}\pi^-$ enhancement

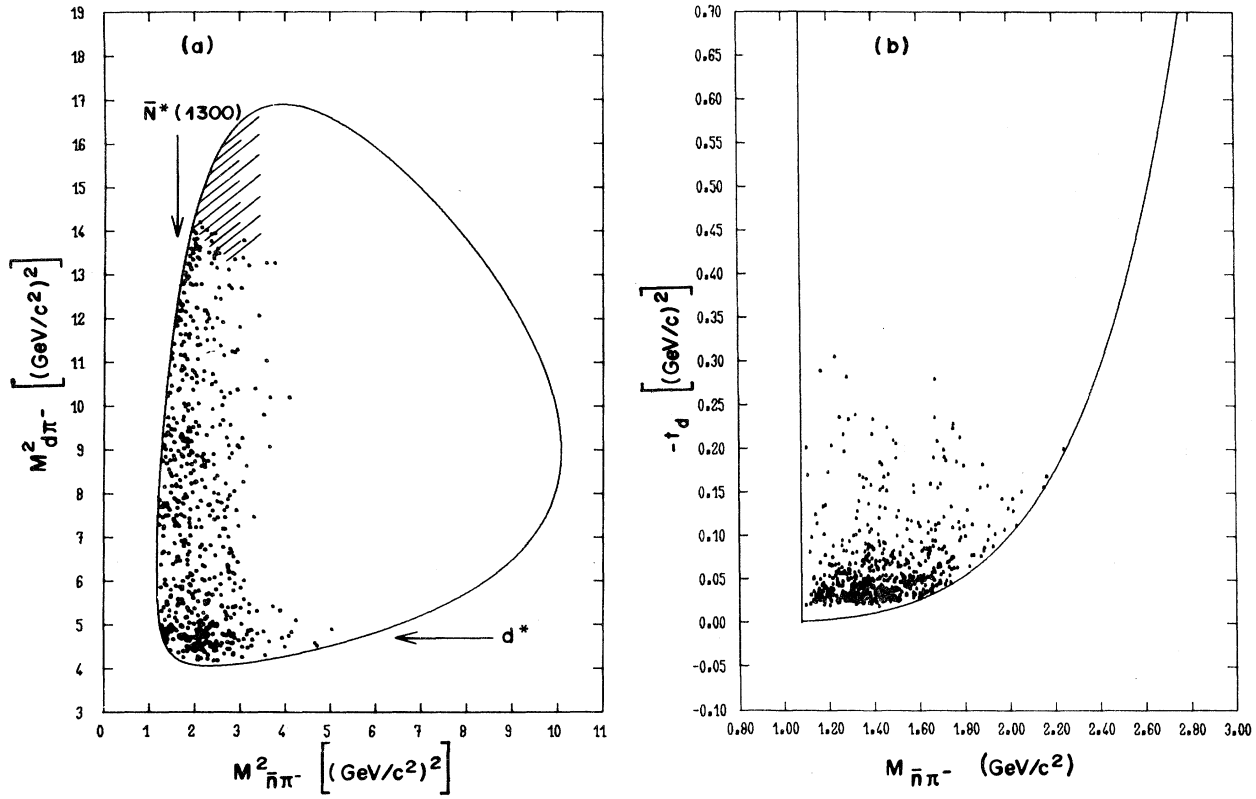

FIG. 1. (a) The Dalitz plot for the $\bar{p}d \to \bar{n}d\pi^-$ reaction. The shaded area in this plot indicates the region in which 27 ± 7 events were lost because of our $p_{\pi}^{\text{lab}} > 3$ GeV/c cut. (b) The Chew-Low plot. For $|t_d| \lesssim 0.02$ (GeV/c)^2 the events have too short an outgoing deuteron track to be recorded at the scanning level.

observed at ~1.3 GeV/c^2 and which will be discussed in Sec. IV.

III. CROSS SECTION

To calculate the cross section we corrected our sample for scanning losses. This was essentially made by correcting the $t' = |t_d - t_{d\,\min}|$ distribution where $t_{d\,\min}$ is the smallest allowable $|t_d|$ value for a given mass of the $\bar{n}\pi^-$ system. In the $t' > 0.02$ (GeV/c)^2 region the correction was obtained from the study of the azimuthal distribution of the outgoing deuteron tracks around the incident $\bar{p}$ beam for different t' bands. For $t' \leq 0.02$ (GeV/c)^2 the losses are too important to apply such a correction. Therefore we estimated these losses by assuming that the t' distribution for $t' \leq 0.02$ (GeV/c)^2 presents the same exponential behavior as in the $0.02 < t' < 0.12$ (GeV/c)^2 region. Fitting the experimental distribution in this region with an $e^{b't'}$ function, we obtain $b' = 39.9 \pm 2.3$ (GeV/c)$^{-2}$. Taking then into account the losses due to our P_{π}^{lab} cut, the path-length attenuation due to other competing reactions and the scanning efficiency of the operators, we obtain a $\bar{p}d \to \bar{n}d\pi^-$ cross section of about 0.92 ± 0.10 mb.

Table I summarizes all the cross sections found in this experiment for reactions having an unbroken deuteron in the final state. Although we dispose of only fitted channels we see that the coherent production cross section is a strongly decreasing function of the number of outgoing particles.

IV. SEARCH FOR RESONANCE PRODUCTION

Figure 1(a) presents the Dalitz plot for the 595 events. The concentration of events in the left-hand side of this plot (i.e., corresponding to small

TABLE I. Summary of the coherent cross sections obtained at 5.55 GeV/c from the present experiment.

Reaction	Cross section
$\bar{p}d \to \bar{p}d$	20.4 ± 4.5 [a] mb
$\bar{p}d \to \bar{n}d\pi^-$	0.92 ± 0.10 mb
$\bar{p}d \to \bar{p}d\pi^+\pi^-$	0.22 ± 0.02 [b] mb
$\bar{p}d \to \bar{p}d\pi^+\pi^-\pi^0$	57 ± 16 μb
$\bar{p}d \to \bar{n}d\pi^+\pi^-\pi^-$	26 ± 8 μb

[a] See Ref. 2.
[b] See Ref. 12.

$\bar{n}\pi^-$ effective-mass values) is a reflection of the strong peripherality of the studied reaction. This can be seen for instance from the Chew-Low plot presented in Fig. 1(b). The lack of events in the $|t_d| \lesssim 0.02$ (GeV/c)^2 region of this plot is due to scanning misrecording of events having short or invisible outgoing deuteron tracks. By comparing our data with the predictions of the various models described below, we always took into account the losses in the $|t_d| \lesssim 0.02$ (GeV/c)^2 region as well as the influence of our P_π^{lab} cut.

In Fig. 2(a) and Fig. 2(b) we present the distributions of the effective masses of the $\bar{n}\pi^-$ ($M_{\bar{n}\pi^-}$) and $d\pi^-$($M_{d\pi^-}$) systems. One notices from these figures the broad $\bar{n}\pi^-$ enhancement around 1.3 GeV/c^2, the so-called N^*(1300), and a $d\pi^-$ bump at 2.18 GeV/c^2 corresponding to the d^* effect.[3] In previous papers[2,4] we discussed in detail this d^* which was interpreted as resulting from a virtual pion exchanged in the t channel which scatters off the deuteron. Despite the fact that the d^* is not a real resonance, its mass spectrum in the vicinity of 2.18 GeV/c^2 has been rather well described by a Breit-Wigner function.[2] This is also the case of the $M_{d\pi^-}$ spectrum shown in Fig. 2(b). This distribution was fitted with an incoherent mixture of peripheral phase space and a Breit-Wigner function giving the central value and width of 2.16± 0.01 and 0.16± 0.04 GeV/c^2, respectively. The fitted curve (full curve in Fig. 2(a) describes adequately the experimental $M_{d\pi^-}$ distributions.

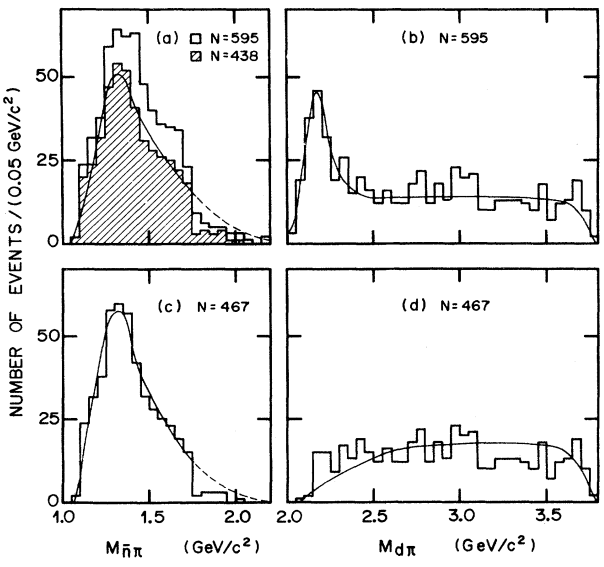

FIG. 2. The $M_{\bar{n}\pi}$ and $M_{d\pi}$ distributions for all the events [(a) and (b)] and distributions obtained by using the "hemisphere" selection [(c) and (d)]. The shaded area in (a) corresponds to events having $M_{d\pi} > 2.3$ GeV/c^2. The full curves in (a), (b), and (c) are obtained by fitting the mass spectra with a Breit-Wigner function and peripheral phase space modified according to our selection criteria. The dashed lines are the predictions outside of the fitted range. In (d) the curve represents the modified phase-space prediction.

The $\bar{n}\pi^-$ enhancement is seen more clearly when we remove the d^* events defined here as $M_{d\pi^-} < 2.3$ GeV/c^2 [shaded histogram of Fig. 2(a)]. The 1.3 GeV/c^2 enhancement has also been observed in other production experiments, but no evidence about its existence has been reported from a phase-shift analysis. In particular, the reactions $K^-p \to \bar{K}\pi N$ at 10 GeV/c,[5] $\pi^+p \to \pi\pi N$ at 8 and 16 GeV/c,[6] and $pp \to NN\pi$ at 19 GeV/c (Ref. 7) present a 1.3-GeV/c^2 bump in the isospin $I = \frac{1}{2}$ $N\pi$ mass spectra. In these reactions the study of the N^*(1300) is thus further complicated by the need to perform an isospin analysis. No such difficulty exists in the present experiment because of isospin conservation, which requires that the system recoiling against the deuteron be in a pure $I = \frac{1}{2}$ state. A similar situation occurs in the $pd \to pd\pi^+\pi^-$ reaction at 28 GeV/c (Ref. 8) in which the ~1.3 bump has also been observed.

To study further the N^*(1300) we also removed the d^* events by a "hemisphere" selection, namely, by choosing only events where the π^- is emitted in the forward c.m. hemisphere. As the emitted $\bar{n}$ and d are strongly collimated along the beam direction, the choice of forward π^- events will tend to suppress the low $M_{d\pi^-}$ mass value and hence the d^* events. Figure 2(d) shows that this selection is indeed efficient. Furthermore this selection procedure has the advantage of not cutting all the events in the N^*(1300)-d^* overlap region of the Dalitz plot. In Fig. 2(c) we present the $M_{\bar{n}\pi^-}$ distribution obtained from the 467 events selected according to the hemisphere criterion. The 1.3 GeV/c^2 bump observed in this figure is not significantly different from that obtained by removing the d^* events with the $M_{d\pi^-} < 2.3$ GeV/c^2 mass cut. We fitted both distributions with an incoherent mixture of Breit-Wigner functions and peripheral phase space deformed according to our selection criteria. The full curves in Fig. 2(a) and Fig. 2(c) represent the fitted distributions, while the results obtained from our fit are given in Table II. One notices from this table the large values for the width as well as the shift toward the low masses of the central values found from these fits. Nevertheless, in contrast to results deduced from various isospin analyses[5-7] the Breit-Wigner shape gives a rather satisfactory description of the present $\bar{n}\pi^-$ enhancement.

V. PRODUCTION MECHANISM

The fact that the N^*(1300) has not been observed in phase-shift analysis suggests considering this

TABLE II. Results obtained by fitting the $M_{\bar{n}\pi}$ distributions with an incoherent mixture of a Breit-Wigner function (having M_0 and Γ as central value and width) and peripheral phase space.

d^* excluded by:	$M_{\bar{n}\pi}$ range used for the fit (GeV/c^2)	M_0 (GeV/c^2)	Γ (GeV/c^2)	Confidence level of the fit (%)
mass cut	1.10–1.75	1.27 ± 0.03	0.25 ± 0.07	47
"hemisphere" selection	1.10–1.80	1.25 ± 0.03	0.32 ± 0.09	60

enhancement as arising from a diffraction-dissociation mechanism. Then apart from spin and parity, the quantum numbers of the $N^*(1300)$ has to be equal to those of the incoming nucleon. This is precisely the case here, where the $\bar{n}\pi^-$ system is produced coherently and has then the quantum numbers of the incoming $\bar{p}$. Although our statistics are not very high, we will investigate if the present data are compatible with some definite spin assignment for the $\bar{n}\pi^-$ enhancement. We examined therefore the so-called $\cos\bar{\theta}$ and $\bar{\varphi}$ decay angular distributions of the π^- in the Gottfried-Jackson frame ($\cos\bar{\theta}_{GJ}$, $\bar{\varphi}_{GJ}$) and in the helicity frame ($\cos\bar{\theta}_H$, $\bar{\varphi}_H$). The Z_{GJ} (Z_H) axis is defined by the incoming $\bar{p}$ (opposite to the outgoing d) direction as seen in the rest frame of the $\bar{n}\pi^-$ for the Gottfried-Jackson (helicity) system, while the normal to the production plane defines the Y axis (the X axis is chosen to give a right-handed coordinate system). These distributions are presented in Fig. 3 for the events selected according to the hemisphere criterion. The shaded area represents those events which are also in the $1.25 < M_{\bar{n}\pi^-} < 1.4$ GeV/c^2 band.

We checked that the scanning losses corrected by a similar method as for the t' distribution did not change the behavior of the distributions shown in Fig. 3. Likewise using Monte Carlo $\bar{p}d \to \bar{n}d\pi^-$ events, we also observed that the P_π^{lab} cut applied to our data (see Sec. II) has no effect on the shape of the angular distributions of the π^-. From Fig. 3 we observe that the angular distributions in the Gottfried-Jackson frame and the helicity system are nearly equal. This is due to the small $|t_d|$ value involved in the coherent $\bar{p}d \to \bar{n}d\pi^-$ reaction which yields somewhat aligned Z_{GJ} and Z_H. Indeed, Fig. 4 shows that the $\cos\theta'$ distribution, θ' being the angle between the Z_t and Z_H axes, obtained from the 467 events is strongly peaked toward $\cos\theta' = 1$.

For a definite spin-parity value of the $\bar{n}\pi^-$ bump, the decay angular distributions have to present some symmetry properties if interference effects with the background can be neglected. Parity conservation for the production process predicts that the distributions of $\cos\bar{\theta}_{GJ}$ and $\cos\bar{\theta}_H$ have to be symmetrical around zero, while the azimuthal $\bar{\varphi}_{GJ}$ and $\bar{\varphi}_H$ distributions must present a symmetry around π.[9] This is verified by the present data, as can be seen from Fig. 3(a) and Fig. 3(b) (shaded area) and from the $\bar{\varphi}_{GJ}$ and $\bar{\varphi}_H$ distributions (not shown) plotted in the interval 0–2π. Furthermore parity conservation in the decay process requires that the $\bar{\varphi}_{GJ}$ also be symmetrical around $\frac{1}{2}\pi$. The $\bar{\varphi}_{GJ}$ distribution folded around π [shaded area of Fig. 3(c)] does not really present this $\frac{1}{2}\pi$ symmetry. However, as stated above, this asymmetry may be due to interference phenomena and thus does not really rule out the resonance interpretation.

We also investigated if the $\bar{n}\pi^-$ enhancement does not simply result from a peripheral type of pro-

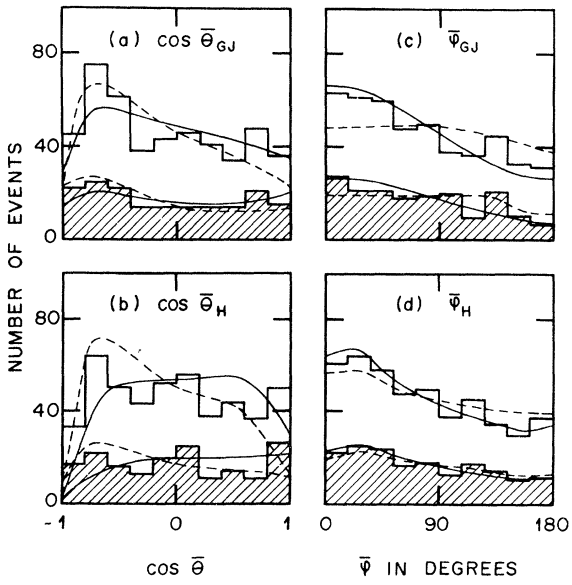

FIG. 3. Angular distribution of the π^- in the Gottfried-Jackson ($\cos\bar{\theta}_{GJ}$, $\bar{\varphi}_{GJ}$) and helicity ($\cos\bar{\theta}_H$, $\bar{\varphi}_H$) frames. The distributions were obtained from the events chosen according to the hemisphere selection, while the shaded histograms correspond to the events which are in addition in the $1.25 < M_{\bar{n}\pi} < 1.40$ GeV/c^2 band. The dashed and full curves are the predictions given by the peripheral and double-Regge-pole model, respectively (see text).

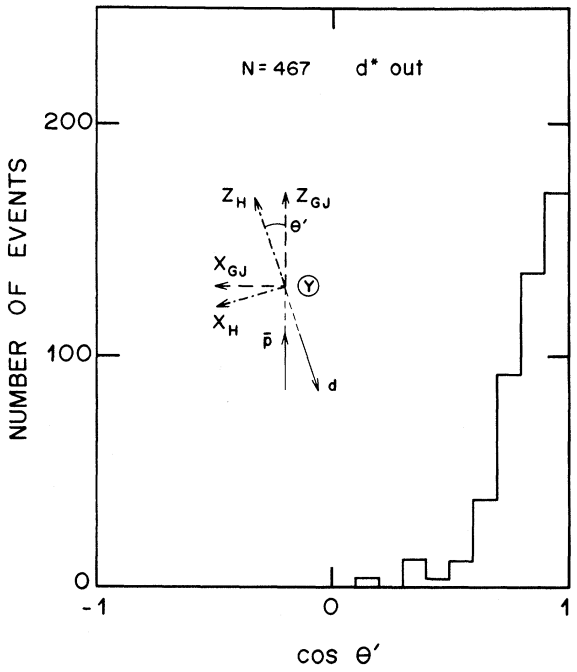

FIG. 4. Distribution of $\cos\theta'$ for the events chosen according to the hemisphere selection. The definitions of the coordinate systems in the Gottfried-Jackson (X_{GJ}, Y, Z_{GJ}) and the helicity (X_H, Y, Z_H) frames are given in this figure. The $\bar{p}$ and d arrows denote the incident $\bar{p}$ and outgoing deuteron momenta as seen in the $\bar{n}\pi^-$ rest system.

duction mechanism. To this end we considered the two models described by the diagrams shown in Fig. 5. In diagram A we assume that a Reggeized pion exchanged in the t channel scatters off the deuteron, yielding then the following matrix element squared:

$$|M_1|^2 = \frac{N|t_1|}{1-\cos[\pi\alpha_\pi(t_1)]}\left(\frac{S_{\bar{n}\pi}}{S_0}\right)^{2\alpha_\pi(t_1)}|T_{\pi d}|^2 .$$

Here $S_{\bar{n}\pi} = M_{\bar{n}\pi}{}^2$, $\alpha_\pi = \alpha'(t_1 - m^2)$ is the pion trajectory, α' its slope taken as 1.13 $(\mathrm{GeV}/c)^{-2}$, m the pion mass, and t_1 the four-momentum transfer between the incident $\bar{p}$ and the outgoing $\bar{n}$; S_0 denotes the scaling factor, N is a normalization constant, while $T_{\pi d}$ represents the elastic πd scattering amplitude.

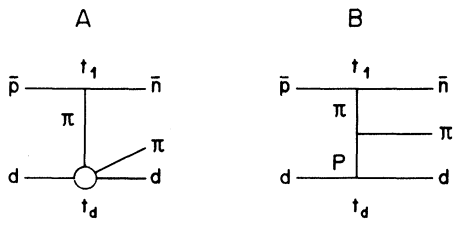

FIG. 5. Diagrams which may contribute to the production of the reaction $\bar{p}d \to \bar{n}d\pi^-$. Diagram A describes a peripheral type model, and diagram B a double-Regge-pole model (see text).

Let us emphasize that such a model was able to reproduce the d^* enhancement in the $\bar{p}d \to \bar{p}d\pi^+\pi^-$ reaction in which πN phase shifts were used to describe the $T_{\pi d}$ amplitude.[2,4] Here, because of our selection procedure which suppresses the events with low $M_{d\pi}$ values, we describe the elastic πd scattering by a diffraction formula; i.e., $T_{\pi d} \sim e^{Bt_d/2}$. A maximum-likelihood fit to our data in the four-dimensional space formed by the variables $M_{\bar{n}\pi}$, $M_{d\pi}$, t_1, and t_d permits us to fit the S_0 and B parameters. These are found to be $S_0 = 2.5$ $(\mathrm{GeV}/c^2)^2$ and $B = 25$ $(\mathrm{GeV}/c)^{-2}$. The dashed curves in Fig. 3 and Fig. 6 represent the results of this fit. Apart from the $M_{\bar{n}\pi}$ distribution, these dashed curves give a rather satisfactory description of the data. Let us also note that the $B = 25$ $(\mathrm{GeV}/c)^{-2}$ found here is nearly equal to those obtained from the diffractive part of the πd elastic differential cross section at 3.65 GeV/c.[10]

We have also considered a double-Regge-exchange model (diagram B of Fig. 5) in which a Pomeranchukon is exchanged at the lower vertex. The matrix element squared which we took is not

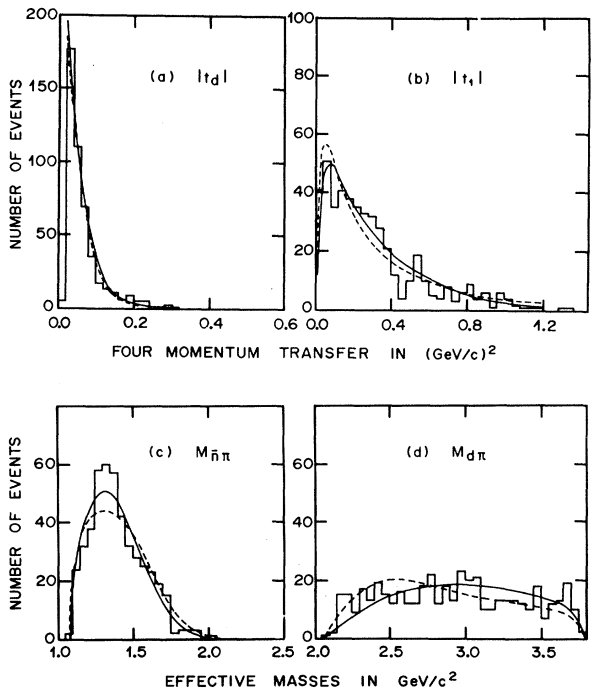

FIG. 6. The $|t_d|$, $|t_1|$, $M_{\bar{n}\pi}$, and $M_{d\pi}$ distributions obtained from the 467 events chosen according to the hemisphere selection. The full and dashed curves represent the fitted distributions obtained from the peripheral and double-Regge-pole model, respectively (see text).

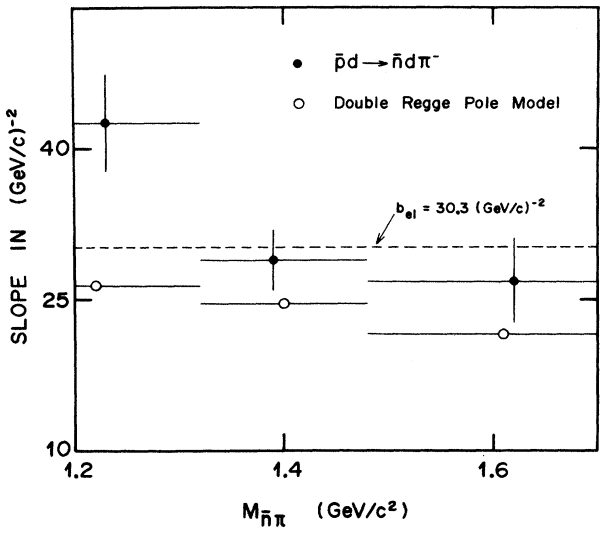

FIG. 7. Slopes obtained from the data and the predictions of the double-Regge-pole model. These slopes are got by fitting the t_d distributions with e^{bt_d} functions in different $M_{\bar{n}\pi}$ bands (see also Table III). The dashed line represents the slope $b_{el} = 30.3 \pm 0.6$ (GeV/c)$^{-2}$ of the elastic $\bar{p}d \rightarrow \bar{p}d$ process.

very different from $|M_1|^2$, i.e.,

$$|M_2|^2 = \frac{N|t_1|}{1-\cos[\pi\alpha_\pi(t_1)]}\left(\frac{S_{\bar{n}\pi}}{S_0}\right)^{2\alpha_\pi(t_1)}(S_{d\pi})^2 e^{Bt_d} .$$

Here e^{Bt_d} is considered as the square of the residue function at the lower vertex and $S_{d\pi} = M_{d\pi}{}^2$.

The maximum-likelihood fit gives $S_0 = 1.2$ (GeV/c^2)^2 and $B = 24$ (GeV/c)$^{-2}$, while the fitted distributions are now given by the full curves shown in Fig. 3 and Fig. 6. As can be seen from Fig. 6(c) the full curve gives a slightly better agreement with the $M_{\bar{n}\pi}$ distribution. Although both models give a rather satisfactory description of the experimental distribution, they are not really able to reproduce entirely the $\bar{n}\pi^-$ bump at ~1.3 GeV/c^2.

VI. DIFFRACTION FEATURES

The diffraction-dissociation mechanism can be observed for a given reaction by studying the variation of its cross section as functions of the c.m. energy. However Satz[11] and also Doren *et al.*[12] predicted that even at a given c.m. energy, there exist some correlation features between M^*, the mass of the dissociatively produced system, and the four-momentum transfer exchanged in the t channel. In these models the momentum-transfer peaking decreases with increasing M^*. Excluding the d^* events by the hemisphere selection, we observed that this behavior is also verified for the present data. This can be seen from Fig. 7, which displays the slopes b of the t_d distributions fitted with e^{bt_d} functions for different $M_{\bar{n}\pi^-}$ bands (see also Table III). The dashed line in this figure indicates the slope obtained from the $\bar{p}d \rightarrow \bar{p}d$ scattering[13] to which, in light of the model of Ref. 11, b has to approach for high $M_{\bar{n}\pi^-}$ values. We also present in this figure the slopes obtained from the double-Regge-pole model. One notes the important disagreement between the calculated slope and the data in the $M_{\bar{n}\pi^-} < 1.32$ GeV/c^2 region. This confirms our previous statement, namely, that the version of the double-Regge-pole model used here is not able to describe all the features of the $\bar{p}d \rightarrow \bar{n}d\pi^-$ reaction.

For diffractive processes it has been conjectured that helicity may be conserved in the s or t channel.[14] Then irrespective of a definite spin assignment of the diffractively produced systems, the azimuthal distributions of the particles coming from these systems have to be symmetrical around the direction for which the helicity conservation holds.[15] Here this implies that for helicity conservation in the Gottfried-Jackson (helicity) frame, the $\bar{\varphi}_{GJ}$ ($\bar{\varphi}_H$) distribution of the π^- has to be isotropic. Figure 3 shows clearly that our data are not compatible with helicity conservation in either the s or the t channel. We checked that the lack

TABLE III. Slopes obtained by fitting the t_d distributions with e^{bt_d} functions for different $M_{\bar{n}\pi}$ bands. The b values are obtained from the data and from the double-Regge-pole model (DRPM).

	Mass band (GeV/c^2)	Mean $M_{\bar{n}\pi}$ value (GeV/c^2)	$\lvert t_d\rvert$ range used for the fit [(GeV/c)^2]	b [(GeV/c)$^{-2}$]
Data	$M_{\bar{n}\pi} < 1.32$	1.23	0.02–0.10	42.6 ± 4.8
	$1.32 < M_{\bar{n}\pi} < 1.48$	1.39	0.02–0.10	29.0 ± 3.0
	$1.48 < M_{\bar{n}\pi}$	1.62	0.04–0.12	26.9 ± 4.2
DRPM	$M_{\bar{n}\pi} < 1.32$	1.22	0.02–0.24	26.4 ± 0.5
	$1.32 < M_{\bar{n}\pi} < 1.48$	1.40	0.02–0.24	24.6 ± 0.5
	$1.48 < M_{\bar{n}\pi}$	1.61	0.04–0.26	21.6 ± 0.4

of isotropy cannot be explained by any of the cuts introduced by our selection procedure. For comparison we present also in Fig. 8 the azimuthal distributions obtained from the $\bar{p}d \to \bar{p}d\pi^+\pi^-$ and $\bar{p}d \to \bar{N}d3\pi$ reactions. For the $\bar{p}d\pi^+\pi^-$ final state we exclude the d^* events and consider only the π^+ distributions, since the $\bar{p}d \to \bar{p}d\pi^+\pi^-$ reaction is dominated by almost 100% $\bar{\Delta}^{--}$ production.[2] In the case of the $\bar{p}d \to \bar{N}d3\pi$ reactions obtained from the $\bar{p}d \to \bar{p}d\pi^+\pi^-\pi^0$ (117 events) and the $\bar{p}d \to \bar{n}d2\pi^-\pi^+$ (52 events) channels, we add the distributions obtained from the three outgoing pions and neglect the influence of the d^* production. As can be seen from Fig. 8(a) and Fig. 8(c) the distributions are very similar to those shown for the $\bar{p}d \to \bar{n}d\pi^-$ reaction (Fig. 3). Thus in any of the coherent $\bar{p}d \to \bar{n}d\pi^-$ and $\bar{p}d \to \bar{p}d\pi^+\pi^-$ reactions produced in this experiment, we do not observe helicity conservation in the s or t channel. For the $\bar{p}d \to \bar{N}d3\pi$ reactions the number of events is too small to draw any certain conclusion.

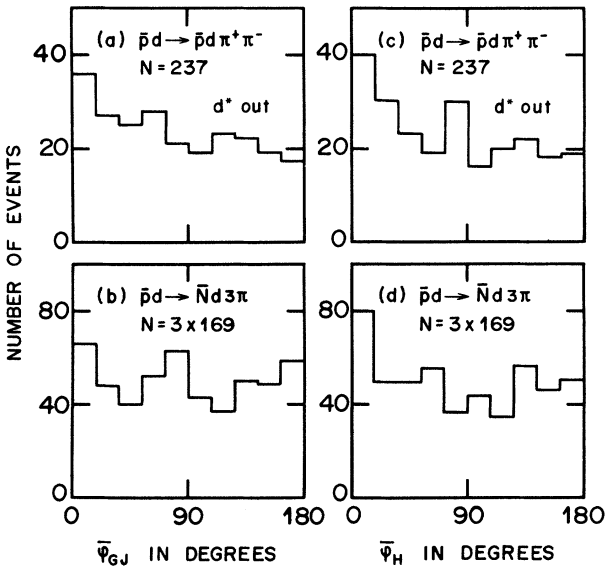

FIG. 8. Azimuthal distributions in the Gottfried-Jackson ($\bar{\varphi}_{GJ}$) and helicity ($\bar{\varphi}_H$) frames of the π^+ and the 3π obtained from the $\bar{p}d \to \bar{p}d\pi^+\pi^-$ and $\bar{p}d \to \bar{N}d3\pi$ reactions, respectively (see text).

VII. CONCLUSIONS

The present data were extracted from a sample of events fitting the $\bar{p}d \to \bar{n}d\pi^-$ reaction. About 5% of the $\bar{p}d \to \bar{n}d\pi^-$ events were lost because of the cut introduced to eliminate the $\bar{p}d \to \bar{p}d\pi^0\pi^0$ contamination. These losses, which correspond approximately to the statistical errors, do not affect the study of the so-called $N^*(1300)$ and d^* enhancements observed in our data.

After correcting our sample for the various cuts applied on our data, we obtained a $\bar{p}d \to \bar{n}d\pi^-$ cross section of 0.92 ± 0.10 mb. A comparison of all the coherent processes obtained from this exposure shows that the coherent cross section is a strongly decreasing function of the number of outgoing particles.

The d^* bump at 2.16 GeV/c^2 and also the $\bar{n}\pi^-$ enhancement at 1.3 GeV/c^2 can be described by Breit-Wigner functions. Although the d^* is not a real resonance, its Breit-Wigner shape around 2.18 GeV/c^2 was already noted, in particular in the $\bar{p}d \to \bar{p}d\pi^+\pi^-$ reaction obtained from the same experiment. For the $N^*(1300)$ our result contrasts with those obtained from experiments which extract from their data the isospin $I = \frac{1}{2}$ mass distributions.

We have also attempted to describe the production feature of the $\bar{p}d \to \bar{n}d\pi^-$ channel, using peripheral-type models. These models give a rather good over-all description of the experimental distributions. However they reproduce only partly the $\bar{n}\pi^-$ enhancement at 1.3 GeV/c^2 and the slopes of the distribution of t_d (the four-momentum transfer between the incoming and outgoing deuteron) plotted for different $M_{\bar{n}\pi}$ bands. Nevertheless in view of the present statistics and the simplicity of the models used, we can consider that an important part of the observed $\bar{n}\pi^-$ enhancement is a reflection of a peripheral type of production mechanism. Further measurement of the $\bar{p}d \to \bar{n}d\pi^-$ cross sections as functions of the c.m. energy will certainly be necessary in order to study the diffraction dissociation properties of this reaction. The present data show, however, that the exponential slope of the distribution of t_d decreases with increasing $\bar{n}\pi^-$ mass as predicted by some diffraction dissociation models.

Excluding the d^* events from our sample, we have also shown that the present data are not compatible with helicity conservation in the s or t channel. A similar result is also obtained for the $\bar{p}d \to \bar{p}d\pi^+\pi^-$ channel at the same incident momentum, while for the $\bar{p}d \to \bar{N}d3\pi$ reaction the statistics are too small to draw any firm conclusion.

ACKNOWLEDGMENTS

It is a pleasure to thank Dr. E. L. Berger and Dr. G. Cohen-Tannoudji for a useful discussion.

*Now at the Centre d'Etudes Nucléaires de Saclay.
†Present address: Physics Department, Case Western Reserve University, Cleveland, Ohio 44106.
‡Present address: The Open University, Bletchley, United Kingdom.
[1]This is a definition slightly different from that used in a previous article; see H. Braun *et al.*, Phys. Rev. D 6, 2311 (1972).
[2]H. Braun, D. Evrard, A. Fridman, J.-P. Gerber, G. Maurer, A. Michalon, B. Schiby, R. Strub, and C. Voltolini, Phys. Rev. D 2, 1212 (1970).
[3]See, for instance, D. Evrard, A. Fridman, and C. Hirshfeld, Nucl. Phys. B14, 699 (1969).
[4]H. Braun, D. Evrard, A. Fridman, J.-P. Gerber, A. Givernaud, R. Kahn, G. Maurer, A. Michalon, B. Schiby, R. Strub, and C. Voltolini, Phys. Rev. D 3, 2572 (1971).
[5]H. Graessler *et al.*, Nucl. Phys. B47, 43 (1972).
[6]K. Boesebeck *et al.*, Nucl. Phys. B40, 39 (1972).
[7]H. Bøggild *et al.*, report submitted to the Fifteenth International High Energy Conference on High Energy Physics, Kiev, 1970 (unpublished).
[8]R. S. Panvini, J. Hanlon, W. H. Sims, J. W. Waters, and T. W. Morris, Nucl. Phys. B39, 538 (1972).
[9]See, for instance, Suh Urk Chung, CERN Report No. CERN 71-8, 1971 (unpublished).
[10]See, for instance, H. C. Hsiung, E. Coleman, B. Roe, D. Sinclair, and J. Vander Velde, Phys. Rev. Lett. 21, 187 (1968).
[11]H. Satz, Phys. Lett. 32B, 380 (1970).
[12]D. Dorren, V. Rittenberg, and D. Yaffe, Nucl. Phys. B30, 306 (1971).
[13]Elastic $\bar{p}d$ scattering at 5.55-GeV/c incident momentum, H. Braun, A. Fridman, E. Jegham, P. Juillot, J. A. Malko, C. Voltolini, G. R. Charlton, W. A. Cooper, and B. Musgrave, Nucl. Phys. B54, 61 (1973).
[14]See, for instance, J. V. Beaupré *et al.*, Nucl. Phys. B47, 51 (1972).
[15]G. Cohen-Tannoudji, J. M. Drouffe, P. Moussa, and R. Reshanski, Phys. Lett. 33B, 183 (1970).

PHYSICAL REVIEW D VOLUME 8, NUMBER 9 1 NOVEMBER 1973

Study of Λ^0 and $\bar{\Lambda}^0$ Final States Produced in 12.7-GeV/c K^+p Interactions*

D. Cohen,† T. Ferbel,‡ P. Slattery, and S. Stone§
Department of Physics and Astronomy, University of Rochester, Rochester, New York 14627
(Received 4 April 1973)

We investigate highly constrained final states involving the production of Λ^0 and $\bar{\Lambda}^0$ particles in K^+p interactions at 12.7 GeV/c. We show that Λ^0 production appears to proceed dominantly through processes which can be regarded as the fragmentation of the target, while $\bar{\Lambda}^0$ production appears to result mainly from beam fragmentation.

INTRODUCTION

In a previous publication concerning inclusive Λ^0 and $\bar{\Lambda}^0$ production in K^+p interactions,[1] we observed that Λ^0 hyperons are produced mainly backward in the center-of-mass system and can thus be regarded as remnants of the breakup of the target proton; $\bar{\Lambda}^0$ antihyperons, on the other hand, are produced mainly forward in this system and conversely can be regarded as resulting from the breakup of the incident K^+ meson. Here we report on the characteristics observed for Λ^0 and $\bar{\Lambda}^0$ particles studied in exclusive final states produced in a 10-event/μb exposure of the BNL 80-in. hydrogen bubble chamber to 12.7-GeV/c K^+ mesons.[2] We consider the following reactions:

$$K^+p \to \Lambda^0 K^+ K^+, \tag{1}$$

$$K^+p \to \Sigma^0 K^+ K^+ \searrow \Lambda^0\gamma, \tag{2}$$

$$K^+p \to \Lambda^0 K^+ K^+ \pi^+\pi^-, \tag{3}$$

$$K^+p \to \Sigma^0 K^+ K^+ \pi^+\pi^- \searrow \Lambda^0\gamma, \tag{4}$$

$$K^+p \to \Lambda^0 K^+ K^+ K^+ K^-, \tag{5}$$

$$K^+p \to \Lambda^0 K^+ \pi^+ K_S^0, \tag{6}$$

$$K^+p \to \Sigma^0 K^+ \pi^+ K_S^0 \searrow \Lambda^0\gamma, \tag{7}$$

$$K^+p \to \Lambda^0 K^+ K^+ \pi^0, \tag{8}$$

$$K^+p \to \bar{\Lambda}^0 ppp, \tag{9}$$

$$K^+p \to \bar{\Sigma}^0 ppp \searrow \bar{\Lambda}^0\gamma, \tag{10}$$

$$K^+p \to \bar{\Lambda}^0 ppp\pi^+\pi^-, \tag{11}$$

$$K^+p \to \bar{\Sigma}^0 ppp\pi^+\pi^- \searrow \bar{\Lambda}^0\gamma, \tag{12}$$

$$K^+p \to \bar{\Lambda}^0 ppp\pi^0, \tag{13}$$

$$K^+p \to \bar{\Lambda}^0 pn\pi^+. \tag{14}$$